ACS APPLIED MATERIALS & INTERFACES

Research Article

www.acsami.org

Selective Sorption of Actinides by Titania Nanoparticles Covalently Functionalized with Simple Organic Ligands

Jessica Veliscek-Carolan,[†] Katrina A. Jolliffe,[‡] and Tracey L. Hanley*[,†]

[†]Institute of Materials Engineering, Australian Nuclear Science and Technology Organisation, Locked Bag 2001, Kirrawee DC, NSW, 2232, Australia

[‡]School of Chemistry, The University of Sydney, NSW, 2006, Australia

Supporting Information

ABSTRACT: Although current and proposed reprocessing of used nuclear fuel is performed predominantly by solvent extraction processes, solid phase sorbent materials have many advantages including the ability to avoid production of large volumes of organic waste. Therefore, three titania nanoparticle based sorbent materials have been developed, functionalized with organic ligands designed to impart selectivity for elements relevant to important separations at the back end of the nuclear fuel cycle. A novel, simplified method of covalent functionalization to the titania surface has been utilized, and the resulting materials have been shown to be hydrolytically stable at pH 2. The sorption behavior of these organofunctionalized titania materials was investigated over a wide pH range with a selection of elements including fission products and actinides. Titania nanoparticles functionalized with an amine or phosphate moiety were able to demonstrate exclusive extraction of uranium under optimized conditions. Titania nanoparticles functionalized with a picolinamide moiety exhibited superior minor actinide sorption properties, in terms of both efficiency and selectivity, to solvent extraction processes using similar organic moieties. As such, organo-functionalized titania materials as solid phase sorbents show promise as a future alternative to solvent extraction processes for nuclear separations.

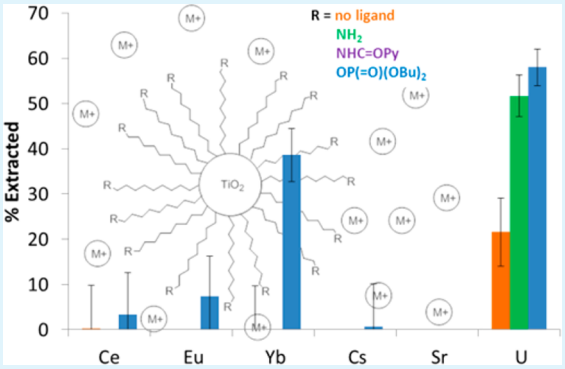

KEYWORDS: *TiO_2, organic funtionalized, sorption, actinide, TBP, picolinamide, amine*

1. INTRODUCTION

The majority of spent nuclear fuel consists of uranium and transuranic elements (plutonium and minor actinides) which have the potential to be transmuted using "Generation IV" reactors such as fast neutron reactors (FNRs).[1] This closing of the nuclear fuel cycle would increase the nuclear lifetime (i.e., the number of years nuclear power will be a viable option for power generation) and decrease the lifetime, radiotoxicity, and volume of nuclear waste requiring long-term storage.[2] Current commercial or proposed reprocessing of used nuclear fuel is performed using solvent extraction techniques. However, the use of solid sorbent materials, as an alternative to solvent extraction, has many advantages, for example, less secondary waste generation (as no organic solvents are required) and faster kinetics in many cases.[3] In addition, the extractant molecule does not need to be soluble in an organic phase, a phase modifier is never required, and there is no possibility of third phase formation. Thus, using solid sorbent materials is likely to reduce the complexity of reprocessing relative to solvent extraction, which in turn reduces the time and cost required. It is therefore of interest to incorporate extractants currently used in solvent extraction processes into solid-phase materials in order to make sorbent materials for separations and nuclear fuel reprocessing.

Several examples exist of organic molecules from solvent extraction processes being incorporated into silica/polymer based ion-exchange materials via intramolecular forces[4,5] or into mesoporous silica materials via covalent silane bonds.[6−8] The main drawback of these silica-based materials for separations in a nuclear context is their chemical instability, both hydrolytic[9] and radiolytic.[10] Group IV metal oxides such as titania demonstrate superior hydrolytic and radiolytic stability.[11] As such, titania based sorbents could also potentially be used, post-sorption, for waste immobilization or as transmutation matrices, since ceramic matrices containing titania are more leach resistant than vitrified silica.[12] Other advantages of titania include ready availability, cost effectiveness, and non-toxicity.

Organo-functionalized group IV metal oxide materials are less common than their silica counterparts, but examples do exist in the literature, particularly for titania in the field of photovoltaics.[11,13,14] In most cases, the desired functional group is anchored to the surface by ionic bonding of phosphate or carboxylate groups,[15,16] with phosphate groups providing superior strength and selectivity for titania than carbox-

Received: September 4, 2013
Accepted: November 1, 2013
Published: November 1, 2013

ylates.[11,13] However, under acidic conditions some grafted phosphate groups are still cleaved from the surface of titania materials.[17] Therefore, this study has explored the possibility of covalent attachment of an organic extractant to the surface of titania via a long-chain alkene,[18] resulting in self-assembly of the aliphatic chains to give good surface coverage and attachment to the titania surface via Ti−O−C bonds that should provide superior stability to hydrolytic cleavage. Using a direct covalent linkage of an alkyl chain to the surface rather than a phosphate anchor group should also allow closer, more ordered packing and hence higher loading of the organic moiety, since the relatively large surface area of phosphonate groups (0.25 nm^2) impedes close packing of the alkyl chains.[19]

Recovery of uranium from nuclear and industrial wastewater is another important and topical area of research due to its heavy metal toxicity and radioactivity.[20] As such, a variety of sorbent materials, including functionalized mesoporous silica,[21] metal-organic frameworks (MOFs),[22] ion-exchange and chelating resins,[23] have been investigated for their uranium extraction properties. Of the amidoxime, imide dioxime, phosphonate, and carboxylate based ligands used for functionalization of mesoporous silica, a phosphonate based material showed the highest U capacity at pH 8.[21] Also, the MOF designed for U extraction utilized a phosphoramidic acid ligand as its organic linker.[22] This demonstrates the well-established high affinity of phosphonate groups for the uranyl cation. However, under different conditions of pH and nitrate concentrations, different resins with either phosphonic acid, carboxylic acid, or amino functional groups were shown to provide the most effective U extraction.[23] Therefore, amine, amide, and phosphate based ligands were used for functionalization of titania in the present study, since titania provides superior hydrolytic and radiolytic stability to silica and polymer-based resins.[24,10]

The sorption behavior of three organo-functionalized titania materials has been investigated using a range of elements relevant to the nuclear fuel cycle (fission products Ce, Eu, Yb, Cs, and Sr as well as actinides U and Am) with varied pH in nitrate media in order to investigate their utility. First, an amine functionality was chosen due to its simplicity and the ability of amines to coordinate many metal species. Second, a novel picolinamide was synthesized, as picolinamides are simple ligands with the potential to achieve the challenging separation of the long-lived and radiotoxic minor actinides from the lanthanide fission products.[25] The minor actinides must be isolated from the highly neutron absorbing lanthanides in order for transmutation into less long lived and radiotoxic elements by neutron capture in FNRs to be possible.[1] Finally, a novel alkylphosphate ligand was synthesized to mimic the behavior of tributyl phosphate (TBP) in the Plutonium and URanium EXtraction (PUREX) solvent extraction process which is used commercially to selectively extract plutonium(IV) and uranium(VI) from a solution of used nuclear fuel dissolved in 3−6 M nitric acid.[26] The selectivity and pH dependence of sorption by these three materials is reported.

2. EXPERIMENTAL SECTION

2.1. Chemicals and Materials. All chemicals were supplied by Sigma-Aldrich, were reagent grade or higher, and were used without further purification. All solvents were distilled before use. The synthesis procedure and characterization of trifluoroacetamide-protected 10-amino-1-undecene (TFAAD) and 1-amino-10-undecene are described in the Supporting Information.

2.2. Preparation of Titania Nanoparticles. Titanium(IV) isopropoxide (35.51 g, 125 mmol) and glacial acetic acid (7.49 g, 125 mmol) were mixed vigorously for 30 s followed by the addition of Milli-Q water (125 mL) to give a white precipitate. The suspension was stirred for a further 30 minutes and then allowed to settle, and the liquid was removed. The solid was then washed with Milli-Q water (5 × 125 mL). After the final wash, the solid was suspended in nitric acid (0.2 M, 125 mL) and stirred for 15 minutes at room temperature and then for a further 24 h at 70 °C, maintaining the volume at approximately 125 mL. The resulting stable sol was decanted into a petri dish and allowed to evaporate to dryness. The resulting solid was ground in a mortar and pestle to give a fine white powder, which was thermally treated at 150 °C for 5 h then at 400 °C for 24 h, both with a ramp rate of 2 °C/min, then heated to 600 °C for 10 minutes, with a ramp rate of 10 °C/min, affording titanium dioxide nanoparticles (8.1 g, 101 mmol).

2.3. Preparation of Novel Organic Ligands. *10-Undecen-1-yl-2-pyridinecarboxamide.* 2-Pyridinecarboxylic acid (0.73 g, 5.9 mmol) and THF (35.0 mL) were combined under nitrogen and cooled to −5 °C in an ice bath. Triethylamine (0.82 mL, 5.9 mmol) and ethyl chloroformate (0.56 mL, 5.9 mmol) were added slowly, and the resulting suspension was stirred for 30 minutes, maintaining a temperature below −5 °C. Crude 1-amino-10-undecene (1.02 g, 6.0 mmol) was added and the reaction mixture stirred for a further 6 h, maintaining a temperature below 0 °C. The reaction mixture was filtered and the white residue rinsed with THF (10.0 mL). The solvent was removed from the combined filtrate and washings under reduced pressure to afford the crude product as a brown oil. Purification by flash chromatography on silica gel (98:2 CH_2Cl_2/MeOH), afforded the pure pyridinecarboxamide as a white crystalline solid (1.25 g, 77 % yield). MS (ESI): *m/z* 275 $[M + H]^+$. ^1H NMR (400 MHz, $CDCl_3$) δ (ppm): 8.54 (d, J = 4.1 Hz, 1H), 8.20 (d, J = 7.8 Hz, 1H), 8.05 (br s, 1H), 7.84 (dt, J = 7.8, 1.7 Hz, 1H), 7.42 (m, 1H), 5.81 (m, 1H), 4.96 (m, 2H), 3.46 (m, 2H), 2.03 (dt, J = 7.2, 6.8 Hz, 2H), 1.63 (m, 2H), 1.45−1.20 (m, 12H). ^{13}C NMR (100 MHz, $CDCl_3$) δ (ppm): 165.5, 151.4, 149.2, 140.7, 138.9, 127.5, 123.8, 115.5, 40.9, 35.2, 31.1, 30.9, 30.8, 30.7, 30.5, 30.3, 28.4. IR (ATR, neat): ν_{max} 3400, 3080, 2930, 2860, 1670, 1620, 1540, 1520, 1470, 1430, 1370, 1280, 1240, 1160, 1090, 1040, 998, 909, 820, 749, 692 cm^{-1}. Anal Calcd for $C_{17}H_{26}N_2O \cdot 0.25H_2O$: C, 73.21; H, 9.58; N 10.04. Found: C, 73.20; H, 9.71; N, 9.85.

Dibutyl 10-Undecen-1-yl Phosphoric Acid Ester. Silver(I) oxide (2.76 g, 11.9 mmol) was added to a solution of dibutyl phosphate (5.00 g, 23.8 mmol) and 11-bromo-1-undecene (2.77 g, 11.9 mmol) in acetonitrile (36 mL). The reaction mixture was stirred vigorously at 40 °C for 24 h, then filtered. Concentration of the filtrate under reduced pressure afforded an opaque pale orange liquid which was dissolved in CH_2Cl_2 (25 mL), washed with Milli-Q water (2 × 15 mL), and dried over sodium sulphate. The solvent was removed under reduced pressure to afford the crude product as an orange liquid. Purification by flash chromatography on silica gel (80:20 CH_2Cl_2/ethyl acetate) afforded the pure alkyl phosphate as a pale yellow oil (4.24 g, 98 % yield). MS (ESI): *m/z* 385 $[M + Na]^+$. ^1H NMR (400 MHz, $CDCl_3$) δ (ppm): 5.83 (m, 1H), 4.98 (m, 2H), 4.04 (m, 6H), 2.06 (dt, J = 7.3, 6.9 Hz, 2H), 1.68 (m, 6H), 1.49−1.35 (m, 8H), 1.35−1.28 (m, 8H), 0.96 (t, J = 7.4 Hz, 6H). ^{13}C NMR (100 MHz, $CDCl_3$) δ (ppm): 139.2, 114.1, 67.7, 67.4, 33.8, 32.3, 30.3, 30.3, 29.5, 29.4, 29.1, 29.1, 28.9, 18.7, 13.6. IR (ATR, neat): ν_{max} 2958, 2927, 2857, 1641, 1463, 1387, 1270, 1021, 999, 907, 728 cm^{-1}. Anal Calcd for $C_{19}H_{39}O_4P$: C, 62.96; H, 10.84; P, 8.54. Found: C, 63.00; H, 10.97; P, 8.42.

2.4. Protocol for Functionalization of Titania Nanoparticles. Dry titania nanoparticles (0.50 g) were mixed with a dry, degassed solution of TFAAD in mesitylene (0.22 M, 3.7 mL) under nitrogen. The resulting suspension was heated in an oil bath at 115 °C for 24 h, with stirring, and then filtered. The residue was washed with petroleum ether (5 mL), methanol (5 mL), and CH_2Cl_2 (5 mL) before drying under a vacuum, affording the functionalized nanoparticles (TiO_2-TFAAD) as a light brown powder (0.42 g). This same methodology was used for functionalization of titania nanoparticles with 10-undecen-1-yl-2-pyridinecarboxamide (TiO_2-pico) and dibutyl

10-undecen-1-yl phosphoric acid ester (TiO_2-TBP). In order to prepare TiO_2-TBP/decene, a dry, degassed solution of dibutyl 10-undecen-1-yl phosphoric acid ester (0.12 g, 0.32 mmol) and 1-decene (0.52 mL, 2.7 mmol) in mesitylene (15.0 mL) was utilized to functionalize dry titania nanoparticles (1.00 g) as described above. Deprotection of TiO_2-TFAAD to TiO_2-NH_2 was achieved by mixing TiO_2-TFAAD (0.42 g) with a 7 wt % solution of potassium carbonate in 70:30 v/v methanol/water (4.0 mL) and stirring at room temperature for 48 h. The reaction mixture was then filtered and rinsed with Milli-Q water (5 mL) and methanol (3 mL). Drying under a vacuum afforded TiO_2-NH_2 as a pale brown powder (0.36 g).

2.5. Protocol for Sorption Experiments. Individual stock solutions of 100 ppm Ce, Eu, Yb, Cs, and Sr and 1000 ppm U (approximately 26 Bq/mg) were prepared using metal nitrate salts of each element and Milli-Q water. Subsamples were then prepared by dilution to 1 ppm, and each subsample was pH adjusted to the appropriate value using nitric acid and/or ammonium hydroxide. To prepare 1 ppm ^{241}Am solution, a 0.57 mL aliquot of the stock solution (2.1 MBq/mL, 3M HNO_3, specific activity ^{241}Am = 118.4 MBq/mg) was diluted to 10 mL and adjusted to pH 3 with ammonium hydroxide. Individual element and competitive batch sorption experiments were performed with pH values ranging between 2 and 7 for TiO_2-NH_2, 3 and 7 for TiO_2-pico, and 1 and 5 for TiO_2-TBP. In the experiments where the TiO_2-NH_2 was pre-equilibrated with nitric acid to pH 3 or 5, pH was measured before both the analyte spike was added and sorption began, as well as after filtration at the end of the 24h sorption experiment. Since there was no significant change in pH (±0.1 pH units), the process of filtration was not considered to affect the pH. Batch sorption experiments were performed using 0.01 g of organo-functionalized titania nanoparticles and 2.0 mL of solution, giving a solid-to-liquid ratio of 200. Each experiment was performed in triplicate and using multiple batches of solid material except the ^{241}Am sorption, which was performed in duplicate and using only one batch of solid material. The solutions and powders were contacted in 20 mL plastic screw-cap vials. Samples were shaken on a horizontal mixer at a constant speed of 140 rpm for a period of 24 h. After sorption, each sample was filtered through an individual 0.45 μm syringe filter and the resulting liquid analyzed by ICP-MS or gamma counting. Initial concentrations before sorption were measured from samples shaken and filtered as described above but in the absence of any sorbent material (as a control), to ensure that metal sorption to the plastic vial or filter did not affect the reported results. Measurements of the controls were the same as the concentrations measured of the original metal solutions that were not shaken and filtered. Percentage extraction and partition coefficients (K_d) were calculated by measuring the concentration of the analyte before and after sorption:

$$K_d = \frac{C_f - C_i}{C_f} \times \frac{V}{m}$$

where C_f is the final concentration of the analyte after sorption (mg/L), C_i is the initial concentration before sorption (mg/L), V is the volume of solution added during the sorption experiment (mL), and m is the mass of sorbent material used (g). Errors in the reported percentage extraction values were calculated from the largest standard deviation of the ICP-MS results. The partition coefficients (mL/g) of particular analytes can then be used to calculate separation factors:

$$\text{Separation Factor } SF_{AB} = \frac{K_d(A)}{K_d(B)}$$

2.6. Characterization. Solution nuclear magnetic resonance (NMR) ^{1}H and ^{13}C spectra of the organic ligands were recorded using a Bruker AV400 NMR Spectrometer using $CDCl_3$ as the solvent. Chemical shifts were measured with respect to TMS. Electrospray ionization mass spectra (ESI-MS) of the novel organic ligands were recorded on a 4000 QTrap AB SCIEX Mass Spectrometer. Fourier Transform Infrared (FTIR) spectra of the organic ligands were obtained on a Nicolet Nexus 8700 FTIR Spectrometer (Thermo Electron Corporation) using the Smart iTR attenuated total reflection (ATR) accessory. Elemental analyses of C, H, N, and P content of organic ligands and the functionalized titania materials were performed by the Microanalytical Unit at the Australian National University (ANU). C, H, and N analysis was performed using a Carlo Erba 1106 analyzer. The sample was combusted, and the gases, after scrubbing and reducing, were separated on a gas chromatography column and measured at the detector. Phosphorus determinations were made after oxidative digestion by comparative UV spectrophotometric measurements of the yellow vanadomolybdophosphate complex. A variety of methods are used for decomposition of the sample to minimize chemical interferences.

X-ray diffraction (XRD) on the titania nanoparticles was measured between 5 and 80° (2θ) using a Panalytical X'Pert Pro. The titania nanoparticles were also characterized by small angle X-ray scattering (SAXS) measurements, performed on a Bruker Nanostar SAXS camera, with three pin-hole collimation for point focus geometry using Cu Kα radiation of wavelength 1.54 Å and a Vantec2000 2D detector. The Brunauer–Emmet–Teller (BET) surface area was measured using an Autosorb iQ Quantachrome instrument with nitrogen gas at 77 K. Scanning electron microscopy (SEM) images were collected of titania nanoparticles deposited on double sided carbon tape and coated with 2–3 nm platinum, using a Zeiss Ultra Plus electron microscope operating at 10 kV.

Cross-polarized ^{13}C–^{1}H solid-state NMR spectra of the functionalized titania materials were recorded on a Bruker Biospin Avance III solids-300 MHz instrument using a Bruker 4 mm double resonance magic-angle spinning (MAS) probehead with a MAS frequency of 12 kHz. Nanoparticle size and zeta potential measurements on the non-functionalized and functionalized titania materials (1 mg/mL) were performed in aqueous media using a Nano Series ZS Zen 3600. Size measurements used Plastibrand 2.5 mL disposable cuvettes (DTS0012), and zeta potential measurements used Malvern folded capillary cells (DTS1061).

Elemental concentrations of solutions before and after sorption were measured using inductively coupled plasma mass spectrometry (ICP-MS). Elemental analysis of samples diluted 1:10 in 3% HNO_3 solutions was performed using a Varian 820-MS instrument. Concentrations of Ce, Eu, Yb, Cs, Sr, and U were measured against internal standards. Reported error values were calculated by assuming 5% error in the average of the duplicate or triplicate measured ICP-MS values, unless the standard deviation of the triplicate samples was greater than 5% of the average, in which case the standard deviation was used. Concentrations of americium-241 (^{241}Am) during sorption experiments were measured using a Wallac Wizard 3″ 1480 automatic gamma counter (PerkinElmer). Americium-241 samples of known concentration were used to calibrate the gamma counter, and the limits of linearity were tested by serial dilution. Reported error values were calculated using the standard deviation of the duplicate samples measured.

3. RESULTS AND DISCUSSION

3.1. Synthesis. Preparation of the titania nanoparticle framework material was achieved via a sol–gel route. The titania nanoparticle sol was synthesized according to the method of Hanley et al.[27] High temperature (600 °C) thermal treatment was then required to ensure a clean nanoparticle surface for the subsequent functionalization step. Ligands for functionalization consisted of an alkene group for attachment to the titania surface; an amine, amide, or phosphate functional group for selective sorption of metal cations; and an aliphatic alkyl chain to act as a linker between these two functional groups and to induce self-assembly of the ligands on the nanoparticle surface. Syntheses of the ligands TFAAD and 1-amino-10-undecene were performed according to the methods of Pfister and Wymann[28] and Sieval et al.,[29] respectively, but with minor modifications (see Supporting Information). The ligand 10-undecen-1-yl-2-pyridinecarboxamide was a novel compound synthesized via a known method for coupling of

2-pyridinecarboxylic acids with amines,[30] and the novel dibutyl 10-undecen-1-yl phosphoric acid ester ligand was synthesized using the previously reported methodology for esterification of phosphates with halides.[31] Attachment of these ligands to the titania nanoparticle surface was achieved using only heat, making this methodology simpler than previous alkene−titania functionalizations which have required the use of UV light.[18]

3.2. Characterization of Titania Nanoparticles. The synthesized titania nanoparticles were characterized using a variety of methods. The crystallinity was measured using XRD (Figure 1), which showed them to contain anatase and rutile.

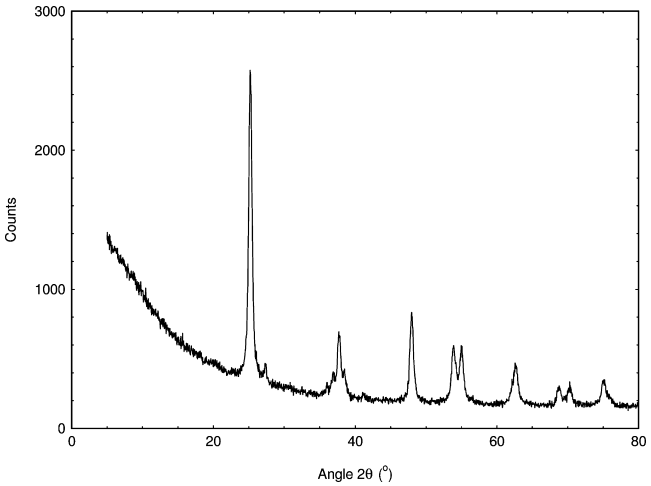

Figure 1. X-ray diffraction pattern of titanium dioxide nanoparticles.

Using the relative intensity ratio (RIR) method,[32] the nanoparticles were shown to contain approximately 10 wt % rutile. The nanoparticle size was calculated according to the Sherrer equation,[33] using the FWHM of the XRD peaks, to give a value of 23 nm. The surface area of the nanoparticles was measured to be 55 mm^2/g.

Particle size was also measured using SAXS and light scattering methods. The SAXS pattern of a solution of titania nanoparticles suspended in Milli-Q water (Figure 2), when fit using SANSView software with a sphere model, indicated the presence of spherical particles of radius 3 nm and a

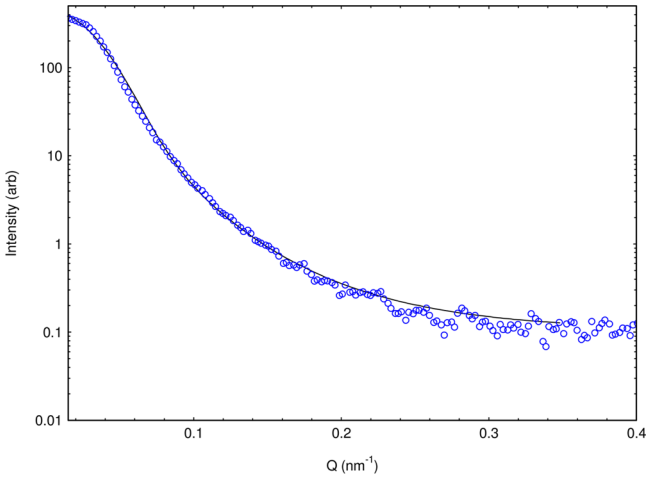

Figure 2. SAXS pattern of titania nanoparticles. Circles = experimental data, line = sphere model fit.

polydispersity index of 0.6. Measurement of the particle size using light scattering (again performed on a solution of titania nanoparticles suspended in Milli-Q water) indicated an average diameter of approximately 500 nm and a polydispersity index of 0.5, with the solution containing particles of two distinct sizes: one with a diameter of 500 ± 150 nm (30% volume fraction) and the other with one of 120 ± 50 nm (70% volume fraction). Thus, it seems that the titania nanoparticles vary widely in size, from small 3 nm diameter particles, which are not seen in the light scattering experiments due to the presence of larger agglomerate particles that produce much higher intensity signals, to larger almost micrometer sized particles, which are too large to see using SAXS.

SEM confirms the presence of a wide distribution of particle sizes (Figure 3). Some of these particles are substantially larger than those that were detected by the methods of SAXS and light scattering, most likely because these larger particles settled out of solution too quickly for measurement by these techniques. The SEM images in Figure 3 also indicate that the large particles (>10 μm) consist of agglomerates of much smaller particles. These smaller particles appear to be approximately 20 nm in size, which is consistent with the particle size determined by the XRD pattern.

3.3. Functionalization of Titania Nanoparticles with Organic Ligands. Solid state $^{13}C-^{1}H$ CP MAS-NMR of non-functionalized titania nanoparticles (TiO_2-NF) as well as titania nanoparticles functionalized with 1-amino-10-undecene (TiO_2-NH_2), 10-undecen-1-yl-2-pyridinecarboxamide (TiO_2-pico), and dibutyl 10-undecen-1-yl phosphoric acid ester (TiO_2-TBP) are shown in Figure 4. Peaks are present in the NMR spectra of TiO_2-NH_2, TiO_2-pico, and TiO_2-TBP which are not present in the spectrum of TiO_2-NF, confirming that functionalization was successful. Peaks with a chemical shift of 10−40 ppm, due to aliphatic carbon,[34] are seen in the NMR spectra of all three functionalized titania materials as all three grafted organic molecules contain alkyl chains. The NMR spectrum of TiO_2-pico also shows peaks with chemical shifts between 110 and 160 ppm, due to aromatic −CH− groups in the picolinamide head group.[34] The peak at approx. 65 ppm in the spectrum of TiO_2-TBP can be assigned as $-CH_2-O$ groups present in the phosphonate head group.[34] The low intensity of the peaks in the NMR spectrum of TiO_2-NH_2 means that the signal due to aliphatic carbon at 20−40 ppm is only just distinguishable from the background. The low intensity in this spectrum relative to TiO_2-TBP and TiO_2-pico may indicate that the level of functionalization is lower for TiO_2-NH_2 or that there is a higher level of mobility in the alkyl chains for this sample. In fact it is likely that a combination of these factors applies as high alkyl chain mobility suggests more space between the attached ligands and hence a lower level of surface coverage.

The level of functionalization of TiO_2-NH_2, TiO_2-pico, and TiO_2-TBP was quantitatively determined by CHN micro-analysis (Table 1). The molecular formulae of the organic functionalized molecules and the total measured %CHN were used to determine the calculated %CHN values, which agreed with the experimentally measured values to within 0.4%. The total organic contents of the organo-functionalized titania nanoparticles were then calculated as the percentage weight of CHNOP but not including water. From this calculation, it was observed that the organic contents of TiO_2-pico and TiO_2-TBP were approximately double that of TiO_2-NH_2, which is consistent with the low signal seen in the NMR spectrum of

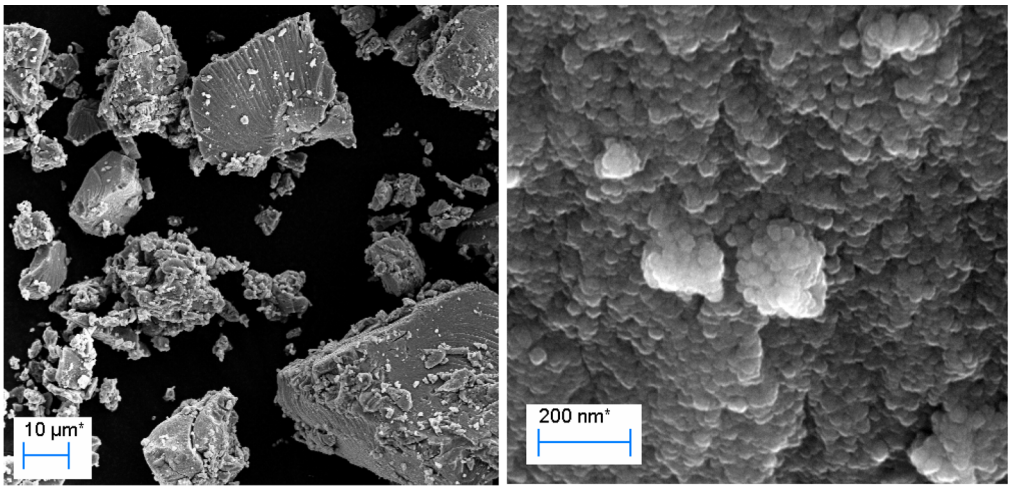

Figure 3. SEM images showing a wide size distribution of agglomerated titania nanoparticles.

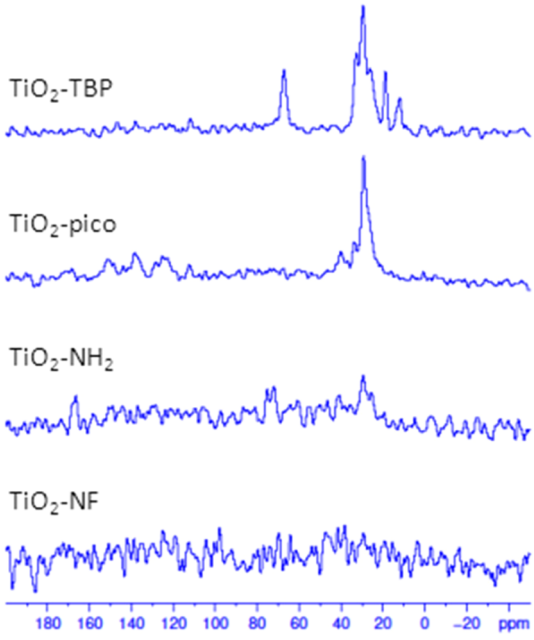

Figure 4. $^{13}C-^{1}H$ CP MAS NMR of organo-functionalized and non-functionalized titania nanoparticles.

Table 1. Elemental CHN Microanalysis of Functionalized Titania Nanoparticles (wt %)

measured	TiO_2-NH_2	TiO_2-pico	TiO_2-TBP
%C	0.5	1.4	1.5
%H	0.3	0.6	0.5
%N	0.3	0.5	0.4
total	1.2	2.5	2.3
calculated	$C_{10}H_{22}N{\cdot}3H_2O$	$C_{17}H_{26}N_2O{\cdot}2H_2O$	$C_{19}H_{39}PO_4{\cdot}H_2O$
%C	0.7	1.6	1.4
%H	0.2	0.3	0.3
%N	0.1	0.2	0.0
total (organic)	0.9	2.2	2.2

TiO_2-NH_2 (Figure 4). However, in terms of molar percentage, the level of functionalization is similar for TiO_2-NH_2 and TiO_2-TBP (0.006 mol %), while that of TiO_2-pico is slightly higher (0.008 mol %). The calculated area per molecule (with a titania nanoparticle surface area of 55 m^2/g) was found to be 1.4 nm^2 for TiO_2-NH_2, 1.5 nm^2 for TiO_2-TBP, and 1.1 nm^2 for TiO_2-pico.

The effect of alkylamine functionalization on the surface charge of the nanoparticles is shown by the zeta potential measurements in Figure 5. In aqueous nitrate media, the

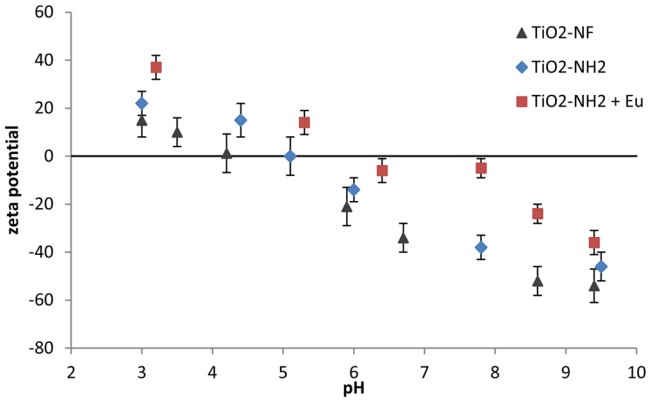

Figure 5. Measured zeta potential of TiO_2-NF in aqueous nitrate media and TiO_2-NH_2 in aqueous nitrate media with and without 1 ppm Eu.

isoelectric points for TiO_2-NF and TiO_2-NH_2 were observed at pH 4.2 and pH 5.0, respectively. The higher isoelectric point of TiO_2-NH_2 is to be expected given that the amino group is basic while the surface of titania consists of both acidic and basic reaction sites. Zeta potential data could not be collected for TiO_2-pico and TiO_2-TBP due to the lack of surface charge on these materials in the pH range of interest (pH 3–7).

3.4. Sorption of Individual Elements with Functionalized Titania Materials. *TiO_2-NH_2.* The ability of TiO_2-NH_2 to sorb Ce, Eu, Yb, Cs, Sr, and U was investigated with metal solutions ranging in pH from 2 to 7. However, it was noted that substantial changes in the pH of the metal solutions occurred after contact with TiO_2-NH_2 if the initial pH was 3 or higher (Table 2); an initial pH of 3 gave a post-contact pH of between 6 and 7, and an initial pH of 4–7 gave a post-contact pH of 8. These results indicate that the TiO_2-NH_2 removed protons from solution and that a protonated amino group (RNH_3^+) was formed. This is not surprising since alkylamine ammonium ions generally have pK_a values between 10 and 11.[35]

Table 2. Measured pH of Filtered (0.45 μm) Nitrate Solutions after Contact with TiO_2-NH_2

initial pH	Ce	Eu	Yb	Cs	Sr	U
2	1.8	1.8	2.5	2.1	2.1	2.0
3	5.8	7.3	6.4	8.1	8.3	7.8
4	7.9	8.1	8.4			7.7
5	8.0	8.1	8.1	8.3	8.3	8.0
7	8.1	8.1	8.1	8.4	8.3	8.1

Since the pH of the sorption solutions increased up to 5 pH units upon contact with TiO_2-NH_2, it was necessary to control the post-contact pH in order to establish the effect of the alkylamine functionalization on sorption behavior and accurately compare the behavior of TiO_2-NF and TiO_2-NH_2. Therefore, sorption experiments were performed, in which nitric acid solutions were pre-equilibrated with TiO_2-NH_2 to pH 3 or 5 before a 100 ppm spike of the analyte of interest was added (to give a final concentration of 1 ppm) and batch sorption performed for 24 h (pH was measured both before and after sorption to confirm no change in pH). The surface charge of TiO_2−NH_2 was negative when the post-contact pH was above 5 (see Figure 5); this is despite sorbed protons due to the high pK_a of the amine functional group. The negative surface charge most likely originated from excess nitrate anions surrounding the protonated TiO_2-NH_3^+ surface. The results of sorption experiments for the non-functionalized titania nanoparticles (TiO_2-NF) and TiO_2-NH_2 are listed in Table 3.

Table 3. Percentage Extraction of 1 ppm Ce, Eu, Yb, Cs, Sr, and U (as Individual Elements) by TiO_2-NF and TiO_2-NH_2[a]

			TiO_2-NF		
pH	2	3	4	5	7
Ce	0	5 ± 9	3 ± 9	79 ± 4	≥ 99.9
Eu	1 ± 9	7 ± 9	7 ± 9	66 ± 4	≥ 99.9
Yb	0	7 ± 9	10 ± 9	47 ± 5	≥ 99.9
Cs	x	0.2 ± 10	x	1 ± 11	1 ± 10
Sr	2 ± 9	5 ± 9	x	15 ± 8	20 ± 8
U	19 ± 8	49 ± 5	x	≥ 99.9	≥ 99.9
			TiO_2-NH_2		
pH	2	3	4	5	6−7
Ce	0	10 ± 15	x	≥ 99.1	≥ 99.8
Eu	0	13 ± 18	x	≥ 99.9	≥ 99.8
Yb	0	2 ± 9	x	99 ± 2	≥ 99.8
Cs	0	0	x	0	14 ± 10
Sr	0	0	x	2 ± 9	98 ± 1
U	29 ± 9	89 ± 15	x	≥ 99.9	99 ± 1

[a]Note varying pH values are measured post-contact. x = not measured.

For TiO_2-NF, sorption of all the metal cations increased with pH, except for Cs, which was not substantially sorbed at any pH. This can be explained by electrostatics since as pH was increased the titania surface charge changed from positive to negative (Figure 5); the metal cations hence went from being repelled by the positive surface to attracted to a negative surface. Uranium was the only element sorbed more than 10 % below the isoelectric point of pH 4.2, most likely due to the formation of anionic U nitrate complexes in solution as the nitrate concentration increases.[36] The existence of inner-sphere U-titania complexes (for both rutile and anatase) has been previously demonstrated both experimentally and theoretically.[37,38] Two surface complexes are possible as the uranyl cation is either coordinated by two bridging oxygen atoms or by one bridging and one terminal oxygen. The prevalence of each complex is dependent upon the conditions of sorption. However, as the acidity of the solution increases, sorption becomes less energetically favorable since no stable inner sphere structures form with fully protonated surface oxygen sites.[38] Therefore, it is observed that U sorption decreases with pH to approximately 20% at pH 2.

For TiO_2-NH_2, sorption of Ce, Eu, and Yb (collectively referred to as LN) can again be explained by the isoelectric point, which in this case is 5.0. In aqueous solution below pH 6, LN exist as trivalent cations,[39] and although at pH 7 some hydrolysis to form $LnOH^{2+}$ cations may occur, the concentration of LN in these solutions, ≤ 0.007 mM, is so low that very little hydrolysis and no precipitation are expected. Therefore, at pH 5, the surface charge is no longer net positive, hence LN cation sorption suddenly increases from <15% at pH 3 to ≥99% at pH 5 (Table 3). The zeta potential results in Figure 5 show that at pH 5 TiO_2-NF has a slight negative charge while TiO_2−NH_2 is essentially neutral. Despite this, TiO_2-NH_2 shows higher LN sorption than TiO_2-NF at pH 5 (see Table 3), indicating that the functionalization of the titania surface with the amine moiety has enhanced its affinity for LN cations. In terms of the mechanism of LN sorption, LN ions are known to form inner sphere nitrate complexes $[LN(NO_3)(H_2O)_n]^{2+}$ and $[LN(NO_3)_2(H_2O)_n]^{+}$ with between 10 and 20% relative abundance in solutions of 0.1 mM $LN(NO_3)_3$ and 0.1 mM HNO_3.[40] These conditions are similar to the sorption conditions in this study; 0.01 mM $Ln(NO_3)_3$ and 0.0001−10 mM HNO_3 (pH 2−7). Therefore, it is possible that LN sorption occurs in this system via coordination of the LN ions to the anionic nitrate species surrounding the protonated TiO_2-NH_3^+. The zeta potential measurements in Figure 5 also indicate that in the presence of Eu, the surface charge by TiO_2−NH_2 was more positive at a given pH than when only water, nitrate, and ammonium ions were present. This provides evidence that Eu has been sorbed onto the surface of the TiO_2-NH_2 via outer-sphere sorption, since zeta potential measures the potential at the outside of the stationary layer of liquid surrounding the charged particle (slipping plane).[41]

For Cs and Sr, no substantial sorption occurred below pH 6−7 with TiO_2-NH_2 (Table 3). Cesium was the most poorly sorbed element investigated, which can be attributed to its larger ionic radius (167 pm versus <103 pm)[42] and lower charge density (+1 versus +3), making it a soft Lewis base with poor affinity for the hard oxygen donors of the nitrate anion.[43] Sorption of Sr at pH 6−7 (98%) was much higher than for Cs (14%) since Sr is more "hard" than Cs, with a higher charge density and smaller ionic radius.

The most interesting result was the sorption of U by TiO_2−NH_2, which increased with pH from approximately 30% at pH 2 to approximately 90% at pH 3 and was quantitative by pH 5 (Table 3). This 90% sorption of U by TiO_2-NH_2 at pH 3 was approximately 75% higher than the TiO_2-NH_2 extraction of any other element at pH 3 and approximately 40% higher than the U extraction of TiO_2-NF at pH 3. TiO_2-NH_2 also extracted U selectively and more efficiently than TiO_2-NF at pH 2, but to a lesser extent. When the pH was increased to 5, both TiO_2-NH_2 and TiO_2-NF demonstrated quantitative U sorption. Since at pH 2 and 3, the TiO_2-NH_2 particles are positively charged (Figure 5), this result suggests that the uranyl cation forms a negatively charged complex with nitrate at these lower pH

values where the relative concentration of nitrate is higher.[36] In fact, previous studies have shown that at the molar U/nitrate ratio present in this study at pH 2, $UO_2(NO_3)_3^-$ is the predominant species in solution, and at a U/nitrate ratio equivalent to pH 3, U is present as approximately 20% $UO_2(NO_3)_2$ and 80% $UO_2(NO_3)_3^-$.[44] Thus, the anionic $UO_2(NO_3)_3^-$ species is present in both these solutions and is able to undergo outer sphere sorption to the positively charged nanoparticle surface.

Overall, the results in Table 3 suggest that functionalization of the titania nanoparticle surface with 1-amino-10-undecene altered its sorption behavior by enhancing LN and particularly U sorption.

TiO_2-pico. The ability of TiO_2-pico to sorb Ce, Eu, Yb, Cs, Sr, U, and Am was investigated from pH 3 to 7, and the results are shown in Table 4. The pH of the solutions after contact with TiO_2-pico was unchanged. TiO_2-pico sorption of LN increased with pH from 5% or less at pH 3 to approximately 90% at pH 7. Cesium and strontium were not sorbed at any pH, while U sorption increased from 50% at pH 3 to 99% at pH 7. The observed trend of increasing LN and U sorption with pH for TiO_2-pico can be explained by the increased concentration of H^+ ions in solution at lower pH, which compete with the metal cations for sorption to the TiO_2-pico surface. Thus, despite the similar trend of increasing sorption with pH for TiO_2-pico and TiO_2-NH_2, the mechanism of sorption is different for TiO_2-pico since its surface is uncharged (see section 3.3). A study of U solvent extraction by picolinamide-based ligands showed that the U is complexed by the carbonyl group of the amide.[45] Therefore, it is likely that a similar mechanism of sorption occurs for LN and U in the present system, as they are both hard Lewis bases with a high affinity for hard oxygen donors.[43]

Table 4. Percentage Extraction of 1 ppm Ce, Eu, Yb, Cs, Sr, U, and Am (as Individual Elements) by TiO_2-pico at Varying pH Values[a]

	TiO_2-pico			
pH	3	4	5	7
Ce	1 ± 10	36 ± 7	84 ± 2	92 ± 6
Eu	5 ± 9	68 ± 6	85 ± 1	89 ± 2
Yb	3 ± 9	69 ± 4	72 ± 4	84 ± 3
Cs	2 ± 9	x	0	0
Sr	x	x	0	0
U	47 ± 5	x	99 ± 1	99 ± 1
Am	20 ± 4	x	x	x

[a]x = not measured.

The sorption efficiencies of TiO_2-NF and TiO_2-pico were similar at pH 3 for all elements and at pH 5 and 7 for U. However, TiO_2-pico showed higher LN sorption at pH 4−5 and lower LN sorption at pH 7 than TiO_2-NF. This suggests that under slightly acidic conditions, the presence of the picolinamide on the titania surface enhanced LN sorption. However, at neutral pH when there are no protons competing for sorption, TiO_2-NF sorbed LN more effectively than TiO_2-pico. Thus, TiO_2-pico is more selective for LN over protons than TiO_2-NF but is also a weaker LN sorbent. TiO_2-pico also showed lower Sr sorption than TiO_2-NF at pH 5−7, suggesting that the picolinamide functionality suppresses Sr sorption.

Since calixarene based picolinamide extractants have previously been used in solvent extraction processes to achieve the challenging actinide−lanthanide separation,[25,46] it was of interest to investigate the separation factor between Am and Eu using TiO_2-pico. *N*-Butyl-2-pyridinecarboxamide was previously shown to be unable to extract Am or Eu without the use of a phase transfer agent at pH 3, but once incorporated onto the lower rim of a calix[6]arene (as 37,38,39,40,41,42-hexakis{3-[pyridine-2-carboxy)amino]propoxy}-*p*-*tert*-butylcalix[6]arene) it demonstrated a separation factor $SF_{Am/Eu}$ of 2.3, although with very low efficiency extraction (K_d's <10).[25] At the same pH of 3, TiO_2-pico sorbed ^{241}Am and Eu with distribution coefficients of 40 ± 9 and 11 ± 1, respectively, giving a separation factor $SF_{Am/Eu}$ of 3.6 ± 1.0 (mean ± standard deviation). Therefore, it can be concluded that under similar conditions, Am sorption by TiO_2-pico demonstrated superior extraction efficiency and selectivity to solvent extraction using picolinamide extractants with or without calixarene scaffolds. Although actinide/lanthanide selectivity is still not well understood, it is postulated to arise from the enhanced covalency of actinide−ligand interactions versus lanthanide−ligand interactions, so that ligands with softer donor atoms such as nitrogen and sulfur have a higher affinity for actinides over lanthanides.[47]

TiO_2-TBP. The ability of TiO_2-TBP to sorb Ce, Eu, Yb, Cs, Sr, and U was investigated from pH 1 to 5. These sorption experiments were performed at a lower pH range than TiO_2-NH_2 and TiO_2-pico because TiO_2-TBP was designed as a solid-phase mimic of the TBP extractant in the PUREX process, which is performed under strongly acidic conditions. However, no sorption of any element was observed at pH 1; therefore, Table 5 shows the sorption behavior of TiO_2-TBP from pH 2 to 5. The pH of the solutions after contact with TiO_2-TBP was unchanged.

Table 5. Percentage Extraction of 1 ppm Ce, Eu, Yb, Cs, Sr, and U (as Individual Elements) by TiO_2-TBP at Varying pH Values[a]

	TiO_2-TBP			
pH	2	3	4	5
Ce	x	2 ± 9	47 ± 5	51 ± 11
Eu	x	5 ± 9	79 ± 3	82 ± 3
Yb	4 ± 9	30 ± 9	94 ± 1	97 ± 1
Cs	x	0	x	2 ± 9
Sr	x	0	x	1 ± 9
U	10 ± 9	72 ± 3	x	99 ± 1

[a]x = not measured.

TiO_2-TBP sorption of LN increased with pH from less than 5% at pH 2 to approximately 50% for Ce, 80% for Eu, and 95% for Yb at pH 5. In fact, from pH 3 to 5, LN sorption by TiO_2-TBP increased across the LN series, with higher extraction efficiencies demonstrated for the heavier Yb. The separation factors were $SF_{Yb/Ce}$ = 23.3 ± 5.2 and $SF_{Yb/Eu}$ = 6.1 ± 1.9 (mean ± standard deviation) and were reasonably consistent across the pH range 3−5. Cesium and strontium were not sorbed at any pH, and U sorption was approximately 10% at pH 2 and then increased to 99% at pH 5. This trend of increasing sorption with pH can be explained similarly to TiO_2-pico since the TiO_2-TBP surface is also uncharged (see section 3.3). Alkylphosphate functionalization enhanced sorption of Ce over TiO_2-NF at pH 4, of Eu at pH 4 and 5, and of Yb at pH 2, 3, 4, and 5. TiO_2-TBP also showed lower Sr sorption than

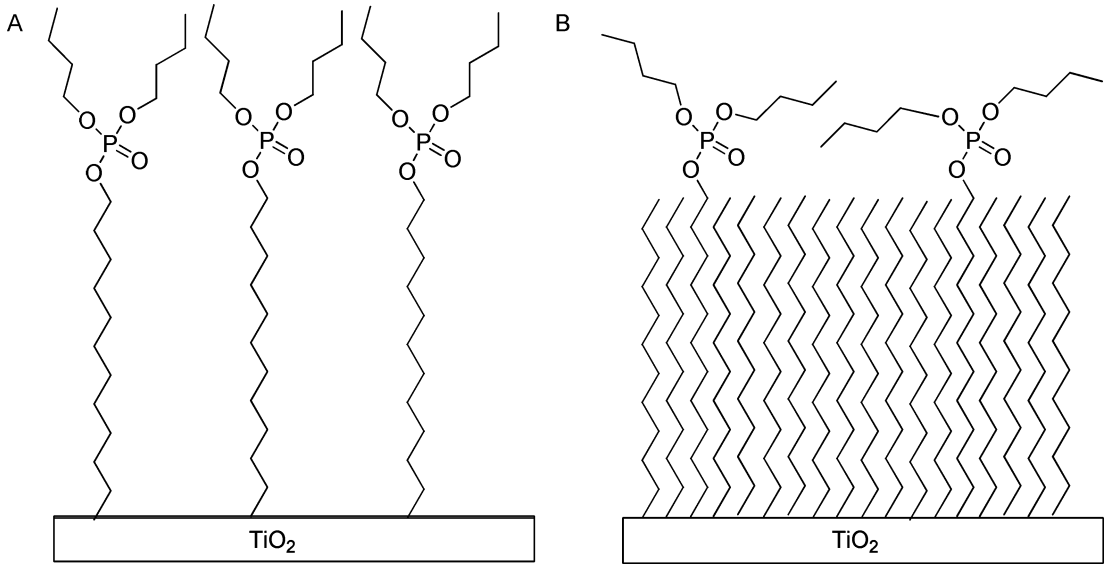

Figure 6. Schematic representation of TiO_2-TBP (A) and TiO_2-TBP/decene (B), illustrating that the oxygen atoms of the phosphate should be more available to coordinate metal ions TiO_2-TBP/decene.

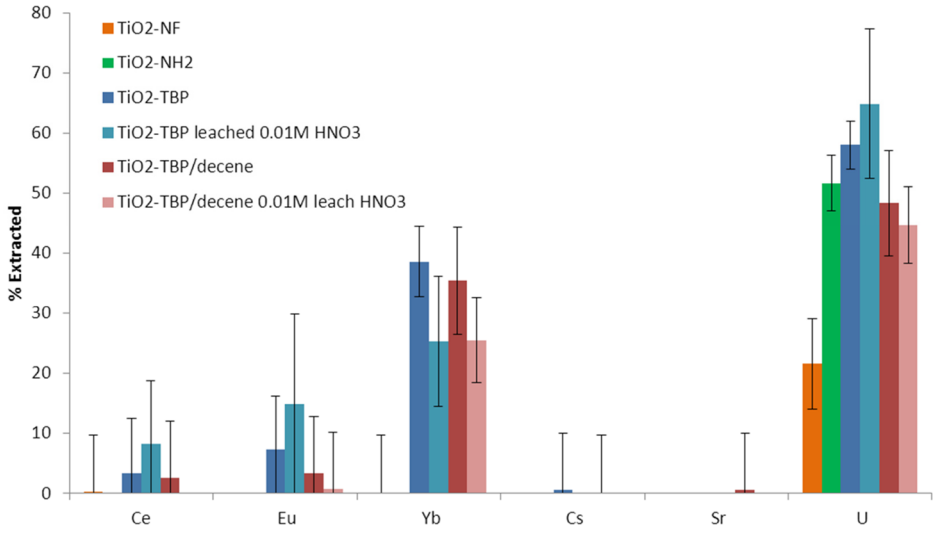

Figure 7. Percentage adsorption of 1 ppm Ce, Eu, Yb, Cs, Sr, and U (competitive) at pH 2.5 for TiO_2-NF, TiO_2-NH_2, TiO_2-TBP, and TiO_2-TBP/decene.

TiO_2-NF at pH 5, suggesting that the alkylphosphate functionality suppresses Sr sorption, similar to TiO_2-pico. Sorption of U was similar for TiO_2-TBP and TiO_2-NF at pH 2 and pH 5, but TiO_2-TBP showed approximately 20% higher sorption of U at pH 3 than TiO_2-NF.

In the PUREX process, TBP is used to selectively extract U and Pu at high acid concentrations (5−6 M HNO_3), and U extraction decreases swiftly with decreasing acid concentration.[48] Therefore, sorption of U from 3 M HNO_3 was investigated to determine whether increased nitric acid concentration would increase U sorption. However, TiO_2-TBP sorption of 1 ppm U was negligible in 3 M HNO_3 (<2%). In order to determine the effect of increasing the nitrate concentration while maintaining an acidity of pH 1 (0.1 M H^+), sorption of U from 0.1 M HNO_3 and 3 M NH_4NO_3 (pH 1) was performed. TiO_2-TBP sorption of 1 ppm U was <1% at pH 1 with a nitrate concentration of 0.1 M (0.1M HNO_3) but increased to approximately 10% at pH 1 when the nitrate concentration was 3 M. As such, increasing nitrate concentration did cause a modest increase in U sorption by TiO_2-TBP, suggesting that nitrate anions are involved in the mechanism of sorption. However, increasing the acid concentration concomitantly removed this effect.

A possible explanation for the low sorption of U by TiO_2-TBP is that the TBP functionality is conformationally constrained when coordinated to the titania nanoparticle surface such that it cannot easily coordinate metal ions from solution (Figure 6A). This hypothesis is supported by the fact that molecular dynamics simulations have shown that during solvent extraction, the TBP of the $UO_2(NO_3)_2(TBP)_2$ complex formed at the aqueous/organic interface is primarily coordinated to UO_2 via the P═O group,[49] which can be seen to be particularly restricted in Figure 6A. It also suggests that the apparent selectivity of TiO_2-TBP for heavier LN could be attributed to their smaller ionic radii (102 pm for Ce, 95 pm for Eu, and 87 pm for Yb),[42] since smaller ions are more likely to be able to approach the sterically hindered P═O group.

dx.doi.org/10.1021/am403727x | ACS Appl. Mater. Interfaces 2013, 5, 11984−11994

Uranium(VI) has an even smaller ionic radius of 73 pm[42] and is therefore extracted more effectively than Yb.

In order to try and improve the extraction efficiency of U, titania nanoparticles were functionalized with dibutyl 10-undecen-1-yl phosphoric acid ester and 1-decene in a 1:10 ratio to give TiO_2-TBP/decene. In this material, the alkylphosphonate groups should have more conformational freedom (Figure 6B). Sorption of U with TiO_2-TBP/decene gave similar extraction efficiencies to TiO_2-TBP (within error) at pH 1−2, but at pH 3 U extraction efficiencies were slightly higher with TiO_2-TBP/decene (86 ± 5 % versus 72 ± 3 %). At pH 5, both materials sorbed approximately 99 % U, and thus their performances could not be distinguished. These results are still not comparable to the solvent extraction of U in the PUREX process. However, the fact that U sorption was similar or greater with TiO_2-TBP/decene than TiO_2-TBP, despite the fact that the number of phosphonate groups on the titania surface is likely to be less for TiO_2-TBP/decene as they are "diluted" by the decene molecules (Figure 6), suggests that the increased conformational freedom of the phosphonate head groups in TiO_2-TBP/decene does enhance their ability to coordinate U ions.

3.5. Competitive Sorption Experiments. It has been shown that TiO_2-NF, TiO_2-NH_2, and TiO_2-TBP extracted U at pH 2 but with low efficiency (approximately 20%). Also, at pH 3, the efficiency of U extraction increased substantially for all three materials, but more for TiO_2-NH_2 and TiO_2-TBP than TiO_2-NF, indicating that the amine and phosphate functionalizations enhanced U sorption. It was therefore of interest to investigate whether selective U extraction could be achieved by TiO_2-NF, TiO_2-NH_2, TiO_2-TBP, and also TiO_2-TBP/decene, during competitive sorption at pH 2.5. TiO_2-pico did not demonstrate enhanced sorption of U relative to TiO_2-NF at pH 3 and was therefore not investigated further. The results of the competitive sorption experiment are shown in Figure 7 and indicate that all four materials demonstrated selectivity for U in a competitive environment, although with varying degrees of efficiency and selectivity.

TiO_2-NF selectively sorbed U from the solution of 1 ppm Ce, Eu, Yb, Cs, Sr, and U but with a low efficiency of only approximately 20%. TiO_2-NH_2, TiO_2-TBP, and TiO_2-TBP/decene all demonstrated a higher U sorption efficiency of approximately 50%, but only TiO_2-NH_2 combined this efficiency with complete selectivity as TiO_2-TBP and TiO_2-TBP/decene also sorbed approximately 35% Yb. Selective sorption of U at pH 2.5 may be of interest in applications such as decontamination of wastewater from mining[50] or dilute low level waste from nuclear processes.[51]

Although examples exist in the literature of organically functionalized titania-based materials being utilized for the sorption of U,[52,53] no selectivity data have previously been reported. The selectivity exhibited by TiO_2-NH_2 at pH 2.5 is superior to other sorbents designed for selective U removal,[54,55] such as a phenolic hydroxyl-functionalized polymer-based chelating sorbent, which during competitive sorption at pH 4.5 sorbed substantial amounts of LNs as well as U. Complete U selectivity has been demonstrated by a fural functionalized mesoporous silica sorbent at pH 5.5,[56] but sorption of U decreased substantially below pH 3, and selectivity at lower pH values was not investigated. TiO_2-NH_2 can also be considered complementary to U/TEVA, a commercially available uranium sorbent consisting of 40 % diamyl amyl phosphonate impregnated in Amberchrom-CG (acrylic ester) resin, which effectively and selectively sorbs U from >1 M acidic solutions.[57] For separations in a nuclear context, a sorbent based on titania also has the advantage of radiolytic stability over silica and polymer based resins.[24,10] The reusability of the materials was not investigated since previous studies have proven the utility of disposal via ceramic wasteforms and the materials produced within this work are of appropriate compositions to be applicable.[12]

3.6. Hydrolytic Stability of Organo-Functionalized Titania Nanoparticle Sorbents. In order to test the hydrolytic stability of these organo-functionalized titania nanoparticle materials, the sorption properties of TiO_2-TBP and TiO_2-TBP/decene were tested before and after leaching with pH 2 HNO_3 for 24 h. If functional groups were lost from the surface during leaching, it would be expected that sorption would decrease and approach the behavior of TiO_2-NF. However, it can be seen from Figure 7 that the extraction efficiencies of TiO_2-TBP and TiO_2-TBP/decene for Yb and U before and after leaching were within error. This suggests that covalent functionalization to the surface of titanium dioxide via an alkene occurs using heat to provide a surface covering that is hydrolytically stable at pH 2 for 24 h.

The hydrolytic stability of TiO_2-TBP and TiO_2-TBP/decene can be considered superior or comparable to other organo-functionalized titania based materials using phosphate groups as anchors for surface functionalization. For example, treatment of mesoporous zirconium titanate frameworks functionalized with methylphosphonic acid with pH 3 HNO_3 for 24 h caused a loss of approximately 10% P.[58] However, increasing the length of the alkyl chain appears to enhance hydrolytic stability, most likely due to self-assembly of a hydrophobic layer on the surface of the framework material, since octadecylphosphonate functionalized titania lost only 5 % of its functional groups after 1 week in a solution of 1:1 HCl/THF (pH 1).[17]

4. CONCLUSIONS

Organo-functionalized titania nanoparticle materials have been synthesized with alkylamine, alkylpicolinamide, and alkylphosphate functionalities covalently attached to the surface via a simple, novel heating methodology. The sorption behavior of these three hybrid materials with elements relevant to important separations at the back end of the nuclear fuel cycle were explored in a wide pH range. Both the amine and phosphate functionalized titania nanoparticles were able to selectively sorb uranium at low pH in a competitive environment, making this study the first reported example of organically functionalized titania based sorbents for the selective sorption of uranium from solution. The excellent selectivity of the amine functionalized titania nanoparticles in particular was remarkable given the simplicity of the ligand. The picolinamide functionalized material also showed superior Am−Eu selectivity to a picolinamide functionalized calixarene extractant in a solvent extraction process. Overall, it has been demonstrated that covalently functionalized titania nanoparticles can be synthesized with simple organic functionalities to provide simple, cost-effective, hydrolytically stable and selective solid-phase sorbents. To increase the utility of these materials into the future, framework materials with greater surface area will be utilized to enable increased loading of the organic ligands and hence improve the capacity and kinetics of sorption.

■ ASSOCIATED CONTENT

Supporting Information

Synthesis methodology for TFAAD and 1-amino-10-undecene. This material is available free of charge via the Internet at http://pubs.acs.org.

■ AUTHOR INFORMATION

Corresponding Author

*E-mail: Tracey.Hanley@ansto.gov.au.

Notes

The authors declare no competing financial interest.

■ ACKNOWLEDGMENTS

The authors gratefully acknowledge Greta Moraes for performing the mass spectrometry analyses; Aditya Rawal and James Hook for provision of solid state MAS-NMR, Joel Davis for provision of SEM, Inna Karatchevtseva for her support with the nanosizer/zeta potential and porosimetry measurements; and Robert Knott for his assistance with the SAXS measurements.

■ REFERENCES

(1) Messaoudi, N.; Tommasi, J. *Nucl. Technol.* **2002**, *137*, 84−96.
(2) Magill, J.; Berthou, V.; Haas, D.; Galy, J.; Schenkel, R.; Weise, H. W.; Heusener, G.; Tommasi, J.; Youinou, G. *Nucl. Energy (Br. Nucl. Energy Soc.)* **2003**, *42*, 263−277.
(3) Hubscher-Bruder, V.; Haddaoui, J.; Bouhroum, S.; Arnaud-Neu, F. *Inorg. Chem.* **2010**, *49*, 1363−1371.
(4) Hoshi, H.; Wei, Y.-Z.; Kumagai, M.; Asakura, T.; Morita, Y. *J. Alloy. Compd.* **2006**, *408-412*, 1274−1277.
(5) Zhang, A.; Hu, Q.; Wang, W.; Kuraoka, E. *Ind. Eng. Chem. Res.* **2008**, *47*, 6158−6165.
(6) Fryxell, G. E.; Mattigod, S. V.; Lin, Y.; Wu, H.; Fiskum, S.; Parker, K.; Zheng, F.; Yantasee, W.; Zemanian, T. S.; Addleman, R. S.; Liu, J.; Kemner, K.; Kelly, S.; Feng, X. *J. Mater. Chem.* **2007**, *17*, 2863−2874.
(7) Yantasee, W.; Fryxell, G. E.; Addleman, R. S.; Wiacek, R. J.; Koonsiripaiboon, V.; Pattamakomsan, K.; Sukwarotwat, V.; Xu, J.; Raymond, K. N. *J. Hazard. Mater.* **2009**, *168*, 1233−1238.
(8) Walcarius, A.; Mercier, L. *J. Mater. Chem.* **2010**, *20*, 4478−4511.
(9) Iler, R. K. *The Chemistry of Silica: Solubility, Polymerisation, Colloid and Surface Properties and Biochemistry of Silica*; Wiley-Interscience: New York, 1979; pp 30−49.
(10) Etienne, M.; Walcarius, A. *Talanta* **2003**, *59*, 1173−1188.
(11) Griffith, C. S.; De Los Reyes, M.; Scales, N.; Hanna, J. V.; Luca, V. *ACS Appl. Mater. Interfaces* **2010**, *2*, 3436−3446.
(12) Donald, I. W.; Metcalfe, B. L.; Taylor, R. N. J. *J. Mater. Sci.* **1997**, *32*, 5851−5887.
(13) Taffa, D. H.; Kathiresan, M.; Walder, L. *Langmuir* **2009**, *25*, 5371−5379.
(14) Rehor, I.; Kubicek, V.; Kotek, J.; Hermann, P.; Szakova, J.; Lukes, I. *Eur. J. Inorg. Chem.* **2011**, *12*, 1981−1989.
(15) Soler-Illia, G. J. A. A.; Azzaroni, O. *Chem. Soc. Rev.* **2011**, *40*, 1107−1150.
(16) Clifford, J. N.; Martinez-Ferrero, E.; Viterisi, A.; Palomares, E. *Chem. Soc. Rev.* **2011**, *40*, 1635−1646.
(17) Marcinko, S.; Fadeev, A. Y. *Langmuir* **2004**, *20*, 2270−2273.
(18) Li, B.; Franking, R.; Landis, E. C.; Kim, H.; Hamers, R. J. *ACS Appl. Mater. Interfaces* **2009**, *1*, 1013−1022.
(19) Gao, W.; Dickinson, L.; Grozinger, C.; Morin, F. G.; Reven, L. *Langmuir* **1997**, *13*, 115−118.
(20) Lopes, C. B.; Lito, P. F.; Cardoso, S.P.; Pereira, E.; Duarte, A. C.; Silva, C.M. In *Ion Exchange Technology II: Applications*; Inamuddin, Luqman, M., Eds.; Springer: New York, 2012; p 249.
(21) Vivero-Escoto, J. L.; Carboni, M.; Abney, C. W.; deKrafft, K. E.; Lin, W. *Microporous Mesoporous Mater.* **2013**, *180*, 22−31.
(22) Carboni, M.; Abney, C. W.; Liu, S.; Lin, W. *Chem. Sci.* **2013**, *4*, 2396−2402.
(23) Phillips, D. H.; Gu, B.; Watson, D. B.; Parmele, C.S. *Water Res.* **2008**, *42*, 260−268.
(24) Chiarizia, R.; Horwitz, E. P. *Solvent Extr. Ion Exch.* **2000**, *18*, 109−132.
(25) Casnati, A.; Della Ca', N.; Fontanella, M.; Sansone, F.; Ugozzoli, F.; Ungaro, R.; Liger, K.; Dozol, J.-F. *Eur. J. Org. Chem.* **2005**, 2338−2348.
(26) Paiva, A.P.; Malik, P. J. *Radioanal. Nucl. Chem.* **2004**, *261*, 485−496.
(27) Hanley, T. L.; Luca, V.; Pickering, I.; Howe, R. F. J. *Phys. Chem. B* **2002**, *106*, 1153−1160.
(28) Pfister, J. R.; Wymann, W. E. *Synthesis* **1983**, 38−40.
(29) Sieval, A. B.; Linke, R.; Heij, G.; Meijer, G.; Zuilhof, H.; Sudholter, E. J. R. *Langmuir* **2001**, *17*, 7554−7559.
(30) Gou, F.-R.; Wang, X.-C.; Huo, P.-F.; Bi, H.-P.; Guan, Z.-H.; Liang, Y.-M. *Org. Lett.* **2009**, *11*, 5726−5729.
(31) Furuta, T.; Torigai, H.; Osawa, T.; Iwamura, M. *J. Chem. Soc., Perkin Trans.* **1993**, *1*, 3139−3142.
(32) Spurr, R.A.; Myers, H. *Anal. Chem.* **1957**, *29*, 760−762.
(33) Patterson, A. *Phys. Rev.* **1939**, *56*, 978−982.
(34) Bovey, F. A.; Jelinski, L.; Mirau, P. A. *Nuclear Magnetic Resonance Spectroscopy*, 2nd ed.; Academic Press: San Diego, CA, 1988; pp 404−405.
(35) McMurry, J. *Organic Chemistry*, 6th ed.; Thomson Learning: Belmont, CA, 2004; p 899.
(36) Ikeda, A.; Hennig, C.; Rossberg, A.; Tsushima, S.; Scheinost, A. C.; Bernhard, G. *Anal. Chem.* **2008**, *80*, 1102−1110.
(37) Vandenborre, J.; Drot, R.; Simoni, E. *Inorg. Chem.* **2007**, *46*, 1291−1296.
(38) Geckeis, H.; Lützenkirchen, J.; Polly, R.; Rabung, T.; Schmidt, M. *Chem. Rev.* **2013**, *113*, 1016−1062.
(39) Baes, C. F., Jr.; Mesmer, R. E. *The Hydrolysis of Cations*; Wiley: New York, 1976; pp 129−137.
(40) Oikawa, T.; Urabe, T.; Kawano, S.; Tanaka, M. *J. Solution Chem.* **2011**, *40*, 1094−1107.
(41) Hunter, R. J. *Zeta Potential in Colloid Science: Principles and Applications*; Academic Press: U. K., 1988.
(42) Greenwood, N. N.; Earnshaw, A. *Chemistry of the Elements*, 2nd ed.; Butterworth-Heinemann: Oxford, U. K., 1998; p 75.
(43) Pearson, R.G. *J. Am. Chem. Soc.* **1963**, *85*, 3533−3539.
(44) De Houwer, S.; Görller-Walrand, C. *J. Alloys Compd.* **2001**, *323-324*, 683−687.
(45) Lapka, J. L.; Paulenova, A.; Alyapyshev, M. Y.; Babain, V. A.; Herbst, R. S.; Law, J. D. *Radiochim. Acta* **2009**, *97*, 291−296.
(46) Galetta, M.; Baldini, L.; Sansone, F.; Ugozzoli, F.; Ungaro, R.; Casnati, A.; Mariani, M. *Dalton. Trans.* **2010**, *39*, 2546−2553.
(47) Lan, J.-H.; Shi, W.-Q.; Yuan, L.-Y.; Li, J.; Zhao, Y.-L.; Chai, Z.-F. *Coord. Chem. Rev.* **2012**, *256*, 1406−1417.
(48) Alcock, K.; Best, G.F.; Hesford, E.; McKay, H. A. C. *J. Inorg. Nucl. Chem.* **1958**, *6*, 328−333.
(49) Ye, X.; Cui, S.; de Almeida, V.; Khomami, B. *J. Phys. Chem. B* **2009**, *113*, 9852−9862.
(50) Douglas, G.B.; Wendling, L.A.; Pleysier, R.; Trefry, M.G. *Mine Water Environ.* **2010**, *29*, 108−115.
(51) Nancharaiah, Y. V.; Joshi, H. M.; Mohan, T. V. K.; Venugopalan, V. P.; Narasimhan, S. V. *Curr. Sci.* **2006**, *91*, 503−509.
(52) Kimling, M. C.; Scales, N.; Hanley, T. L.; Caruso, R. A. *Environ. Sci. Technol.* **2012**, *46*, 7913−7920.
(53) Sizgek, G. D.; Griffith, C. S.; Sizgek, E.; Luca, V. *Langmuir* **2009**, *25*, 11874−11882.
(54) Liu, J.; Li, J.; Yang, X.; Song, Q.; Bai, C.; Shi, Y.; Zhang, L.; Liu, C.; Li, S.; Ma, L. *Mater. Lett.* **2013**, *97*, 177−180.
(55) Liu, Y.; Cao, X.; Hua, R.; Wang, Y.; Liu, Y.; Pang, C.; Wang, Y. *Hydrometallurgy* **2010**, *104*, 150−155.
(56) Yousefi, S. R.; Ahmadi, S. J.; Shemirani, F.; Jamali, M. R.; Salavati-Niasari, M. *Talanta* **2009**, *80*, 212−217.
(57) Horwitz, E. P.; Dietz, M. L.; Chiarizia, R.; Diamond, H.; Essling, A. M.; Graczyk, D. *Anal. Chim. Acta* **1992**, *266*, 25−37.

(58) de los Reyes, M.; Majewski, P.J.; Scales, N.; Luca, V. *ACS Appl. Mater. Interfaces* **2013**, *5*, 4120−4128.